

Research article



Journal of Atoms and Molecules

An International Online Journal

ISSN – 2277 – 1247

SYNTHESIS, CHARACTERIZATION, STEREOCHEMISTRY AND DFT STUDY OF
2-AMINO-4-BENZO[H]CHROMENE DERIVATIVESAhmed Elhenawy^{1,4}, Hany M. Mohamed,^{2,4} Ahmed M. El-Agrody*^{3,4}¹Chemistry Department, Faculty of Science and art, AlBaha University, Mukhwah, AlBaha, K.S.A²Chemistry Department, Faculty of Medicine (Boys Branch), Jazan University, Jazan, Saudi Arabia.³Chemistry Department, Faculty of Science, King Khalid University, Abha, P.O. Box 9004, K.S.A.⁴Chemistry Department, Faculty of Science, Al-Azhar University, 11884, Nasr City, Cairo, Egypt.

Received on: 23-11-2013

Revised on: 16-12-2013

Accepted on: 24-12-2013

ABSTRACT:

Interaction of 4-methoxy-1-naphthol (**1**) with α -cyano-*p*-bromocinnamionitrile (**2a**) and ethyl α -cyano-*p*-bromocinnamate (**2b**) provided 2-amino-4-(4-bromophenyl)-6-methoxy-4*H*-benzo[*h*]chromene-3-carbonitrile (**3a**) and ethyl 2-amino-4-(4-bromophen-yl)-6-methoxy-4*H*-benzo[*h*]chromene-3-carboxylate (**3b**) respectively. Structures of these compounds were established on the basis of IR, UV, ¹HNMR, ¹³CNMR and MS data. Moreover, the stereochemistry and the DFT study are discussed. Using density functional theory geometries have been optimized at DFT\B3LYP with 6-31G* and 6-311G* level of theory, the absorption spectra has been computed by using time dependant density functional theory at TD- DFT\B3LYP with 6-31G* and 6-311G* level of theory. The HOMO-LUMO energy gap of studied systems has been discussed.

KEY WORDS: 4-Methoxy-1-naphthol, α -Cyano-*p*-bromocinnamionitrile, Ethyl α -cyano-*p*-bromocinnamate, 4*H*-benzo[*h*]chromenes, Density functional theory, Stereochemistry.

* Corresponding author

Prof. Dr. Ahmed M. El-Agrody,
Email: elagrody_am@yahoo.com
Tel: +966 530175825

INTRODUCTION:

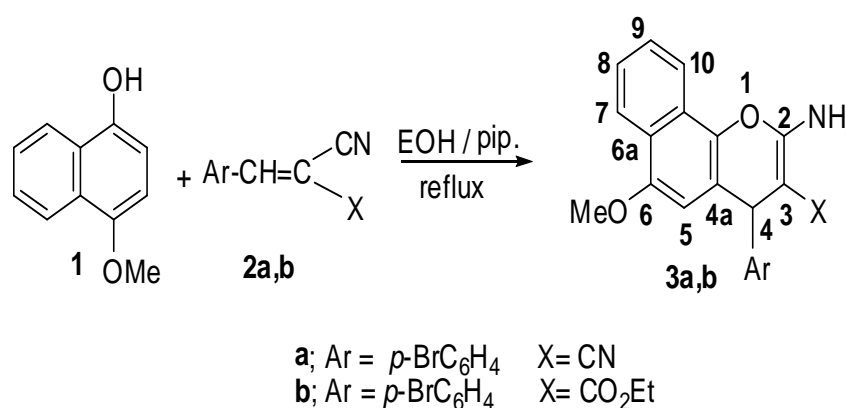
2-Amino-4*H*-benzochromenes are an important class of heterocyclic compounds having important biological activities. During the last decade, such compounds had shown interesting antimicrobial and pharmacological activities [1-42].

In continuation of the previous works [43-57], it seemed interesting to synthesize novel 4*H*-benzo[*h*]chromene compounds using α -cyanocinnamo-nitrile and ethyl α -cyanocinnamate and study their characterization.

Thus, treatment of 4-methoxy-1-naphthol (**1**) with α -cyano-*p*-bromocinnamitrile (**2a**) and ethyl α -cyano-*p*-bromocinnamate (**2b**) in ethanol and piperidine under reflux gave 2-amino-4-(4-bromophenyl)-6-methoxy-4*H*-benzo[*h*]chromene-3-carbonitrile (**3a**) and ethyl 2-amino-4-(4-bromo-phenyl)-6-methoxy-4*H*-benzo[*h*]chromene-3-carboxylate (**3b**) respectively, (Scheme 1).

By applying DFT and TDDFT theories we shed light on the geometries, electronic and

optical properties. The structure-property relationship has been intensively investigated. The compounds which we have studied **3a,b** show stereo isomers *R*-form and *S*-form and also, they have two possibilities, two tautomer amino form and imino form; it was esteemed that imino form would be good as biologically active molecule. Moreover, the effect of NH₂ and NH at position 2 in **3b** (Scheme 3) has been studied.



Scheme 1. Schematic diagram of the new synthesized 4*H*-benzo[*h*]chromene derivatives.

EXPERIMENTAL:

Melting points were determined with a Stuart Scientific Co. Ltd apparatus. IR spectra were determined as KBr pellets on a Jasco FT/IR 460 plus spectrophotometer. ¹H NMR and ¹³C NMR spectra were recorded using a BRUKER AV 500 MHz spectrometer. ¹³C NMR spectra were obtained using distortionless enhancement by polarization transfer (DEPT), with this technique, the signals from CH and CH₃ carbons were positive (up) whilst signals from CH₂ environments are negative (down). Mass spectra were measured on a Shimadzu GC/MS-QP5050A spectrometer. Elemental analyses were performed on a Perkin-Elmer 240 microanalyser in the Faculty of Science Cairo University.

Reaction of 4-methoxy-1-naphthol (1) with 2a,b:

General procedure

A solution of 4-methoxy-1-naphthol (**1**) (0.01 mmol) in EtOH (30 mL) was treated with α -cyano-*p*-bromocinnamitrile (**2a**) or ethyl α -cyano-*p*-bromocinnamate (**2b**) (0.01 mmol) and piperidine (0.5 mL). The reaction mixture was heated until complete precipitation occurred (reaction times: 60 min for **2a**; 120 min for **2b**). The solid product which formed was collected by filtration and recrystallised from ethanol to give **3a,b**. The physical and spectral data of compounds **3a,b** are as follows:

2-Amino-4-(4-bromophenyl)-6-methoxy-4H-benzo[h]chromene-3-carbonitrile (3a)

Pale yellow crystals needles from ethanol; m.p. 218-219 °C; 89%; IR (KBr) ν (cm⁻¹): 3455, 3335, 3270 (NH₂), 3070, 3008, 2973, 2875 (CH stretching), 2191 (CN); ¹H NMR (500 MHz) (DMSO-d₆) δ : 8.20-6.18 (m, 9H, aromatic), 4.78 (s, 1H, H-4), 4.75 (bs, 2H, NH₂), 3.82 (s, 3H, OCH₃); ¹³C NMR (125 MHz) (DMSO-d₆) δ : 159.16 (C-2), 152.44 (C-6), 137.50 (C-10b), 128.34 (C-10a), 126.31 (C-9), 125.49 (C-8), 124.11 (C-6a), 122.27 (C-7), 121.35 (C-10), 120.49 (C-4a), 116.10 (CN), 102.74 (C-5), 60.53 (C-3), 55.68 (CH₃), 41.52 (C-4), 143.37, 131.98, 129.76, 119.76 (aromatic); MS *m/z* (%): 408 (M⁺+2, 43.63), 406 (M⁺, 44.27) with a base peak at 250 (100); Anal. Calcd for C₂₁H₁₅BrN₂O₂: C, 69.52; H, 4.17; N, 7.72. Found: C, 00.00; H, 0.00; N, 00.00 %.

Ethyl 2-amino-4-(4-bromophenyl)-6-methoxy-4H-benzo[h]chromene-3-carboxylate (3b)

Colourless crystals from ethanol; m.p. 160-161 °C; 87%; IR (KBr) ν (cm⁻¹): 3404, 3300 (NH₂), 3010, 2981, 2939, 2899 (CH stretching), 1666 (CO); ¹H NMR (500 MHz) (CDCl₃) δ : 8.17-6.33 (m, 9H, aromatic), 6.41 (bs, 2H, NH₂), 4.97 (s, 1H, H-4), 4.10 (q, 2H, CH₂, *J* = 7 Hz), 3.84 (s, 3H, OCH₃), 1.20 (t, 3H, CH₃, *J* = 7 Hz); ¹³C NMR (125 MHz) (CDCl₃) δ : 169.31 (CO), 160.23 (C-2), 152.01 (C-6), 137.34 (C-10b), 126.98 (C-10a), 125.76 (C-9), 125.08 (C-6a), 124.12 (C-8), 122.13 (C-7), 120.52 (C-10), 119.91 (C-4a), 103.30 (C-5), 78.52 (C-3), 59.52 (CH₂), 55.60 (CH₃), 40.98 (C-4), 14.38 (CH₃), 146.57, 131.21, 129.75, 119.66 (aromatic); MS *m/z* (%): 455 (M⁺+2, 14.22), 453 (M⁺, 15.99) with a base peak at 298 (100); Anal. Calcd for C₂₃H₂₀BrNO₄: C, 67.40; H, 4.92; N, 3.42. Found: C, 00.00; H, 0.00; N, 00.00 %.

Computational detail:

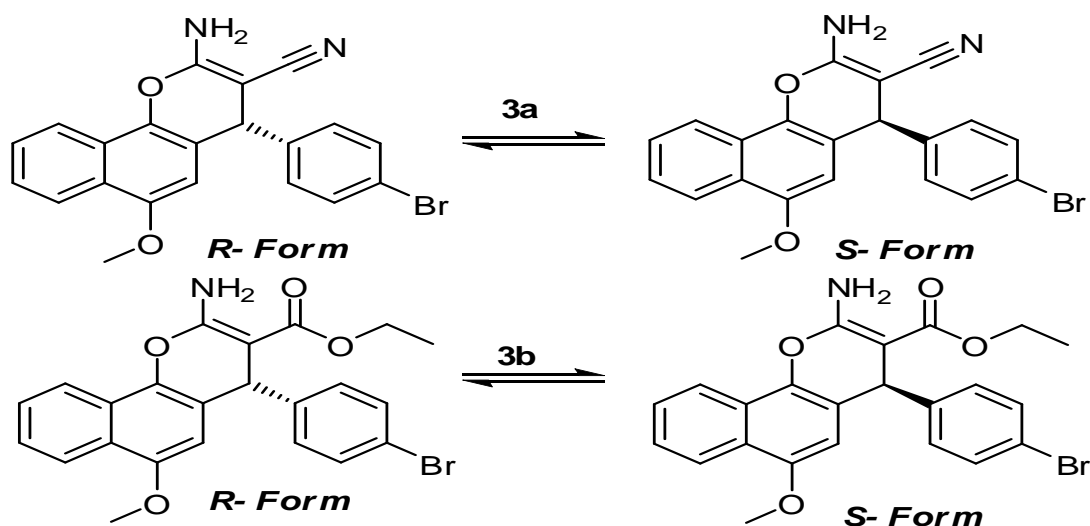
All electronic structure calculations were performed using the Spartan 08 program [58]. Geometry optimizations have been achieved using AM1 semi-empirical molecular orbital for density functional theory [59,60] with a B3LYP/6-31G* and 6-311G* basis sets [59-62]. The structural parameters, such as the dipole moment of the molecules, the energy of the highest occupied molecular orbital EHOMO and the lowest unoccupied molecular orbital ELUMO, atomic charges derive from Mulliken population analysis [63] were obtained. The thermodynamic parameters, including enthalpy (H), entropy (S), Constant volume molar heat capacity (Cv^o), free energy (G), zero-point vibration energy (ZPE).

The absorption spectra and the vibration frequency calculation also, were computed. For each stationary point was performed at DFT with B3LYP/6-311G*, to characterize its nature as minima or transition states and to correct energies. The graphical representation of the molecular electrostatic potential surface (MEP or ESP), as implemented within the SPARTAN program [64,65].

RESULTS AND DISCUSSION

Energy features

Due to the presence of a chiral center, the prepared compounds **3a** and **3b** is possible existence in the two enantiomer forms depicted in (Scheme 2).



Scheme 2: Stereo isomers of synthesized compounds (**3a** and **3b**).

The calculated molecular parameters have been used to investigate the most stable enantiomer form of the compounds under investigation **3a** and **3b** (Table 1). The

optimized geometry structures of **R** and **S** isomers for **3a** and **3b** represented in (Figure 1).

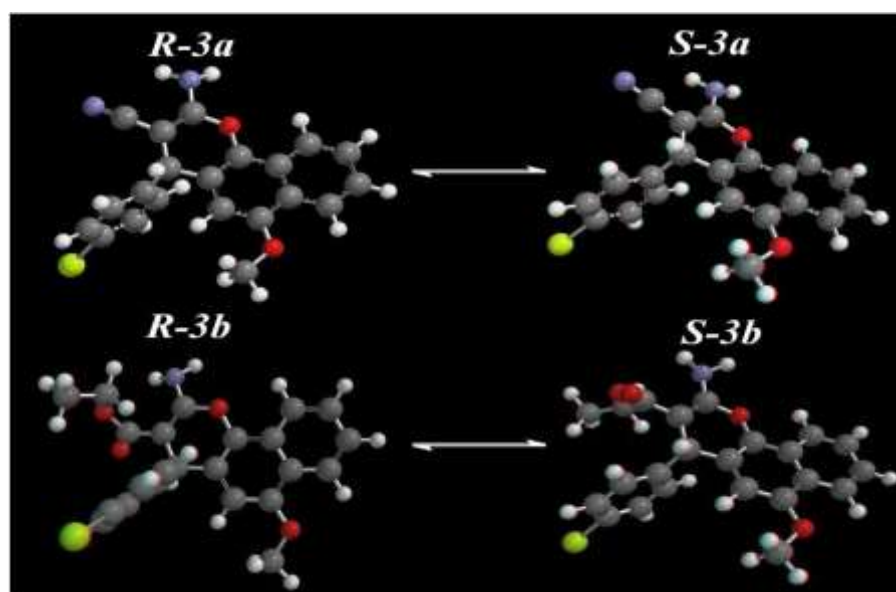
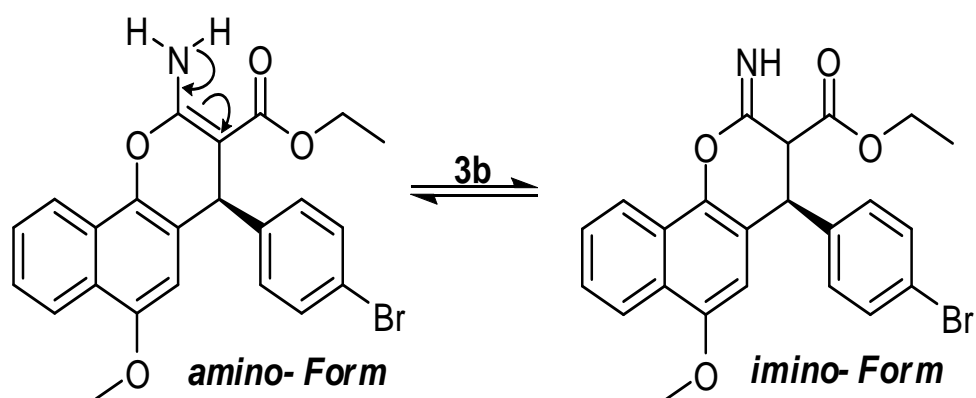


Fig. 1. The lowest energy for stereoisomer of compounds **3a** and **3b** based on DFT B3LYP/6-311G*calculations

The lowering calculated energy of **S** forms compared with **R** forms for **3a** and **3b**, leads to predominance **S** enantiomer form. Also, compound **3b** may be presence in two possible tautomer structures (amino and imino) form represented in (Scheme 3), the

geometrical optimization of both tautomer structures represented in (Figure 2). The amino form is most preferred tautomer structure, due to decreasing energy of the amino form than imino form (Table 1).



Taking into consideration, the zero-point energy at (298.15 K) temperature is the largest for the *R*-**3a** and *R*-imino tautomeric form of **3b**. From comparing the thermodynamic parameters (Table 1), the *S*

enantiomer for **3a** and **3b**, and amino tautomer structure *S*-**3b** more favorable structures, which agrees with the DFT calculations.



Fig. 2. The lowest energy for tautomer structure of **3b** based on AM1 semiempirical by DFT with B3LYP /6-311G* calculations.

Optimized Geometry

In trying to achieve better insight of the molecular structure, the optimization geometry was performed in vacuo with AM1 semi-empirical at DFT/B3LYP quantum mechanical level using 6-311G* set for all synthesized compounds **3a** and **3b** (Figures 1 & 2) and (*S* Figure 1 and Table 2 & 3) in supplementary material). Furthermore, the X-ray single crystal of the most stable compounds *S*-**3a** and amino *S*-**3b** is not available till now, since, the geometrical optimization parameters (bond lengths and

angles) calculated by DFT/B3LYP method with different basis set 6-31G*, 6-311G*, and compared with other till the crystal structures have been solved (Table 2 & 3). In *S*-**3a**, the bromophenyl ring, NH₂ and CN fragments, were arranged in plane with deviation angle (~111°, 125.40 and 179.55), respectively, the bond length C₁-N₂₆ (~1.37 Å). In amino *S*-**3b**, the distance C₄-N₂₇ for amino form (1.462 Å) larger distance than imino form (1.376 Å) see (Table 3) supplementary material, the decreasing bond length for imino form could be explained by

the presence of π electron conjugation of the phenyl ring and the sp^2 hybridization orbitals of *N*-imino which has more *s*-character, and the most electron density is closer to the nuclei compared with the electron density distribution at sp^3 hybridized amino nitrogen, which derive to shortening of the C_4-N_{27} imino bond.

HOMO–LUMO analysis and dipole moments

The frontier molecular orbital's (highest occupied molecular orbital, HOMO and lowest unoccupied molecular orbital, LUMO) are the most important orbitals in a molecule; these orbitals determine the way for the molecule interacts with other species. The HOMO energy values show the donating electron ability of molecule, in other hand, LUMO energy presents the ability of a molecule for receiving electron [66]. The frontier orbital gap; as calculated by simple Hückel Molecular Orbital theory (SHMO) helps to characterize the chemical reactivity and kinetic stability of the molecule [67-69]. The (HOMOs) and (LUMOs) of the studied

systems in the S_0 states have been shown in (Figure 3), which suggests the delocalization and localization of molecular orbital's. The dipole moment, HOMO/LUMO and gap values for all compounds under investigation **3a** and **3b** are given in (Table 4). In general, the *S*-**3a** showed the lowest HOMO energy, *S*-enantiomer structures have lower HOMO energies than corresponding *R*-form for **3a** and **3b**. In addition, nitrogen atoms for CN, NH_2 groups and Oxygen of pyran ring in compound *S*-**3a**, and the O atom of pyran ring for **3b**, are contribute to the HOMO, and donate charge into the ring, and increases the charge at C9 and C4 in the ring, also, the NH_2 function don't contribute significantly to the HOMO (Figure 3). Conversely, the NH_2 and CN groups of *S*-**3a** and NH_2 and O-pyran ring for amino **3b** don't contribute significantly to the LUMO (Figure 3). The overall interpretation of the data suggests that, the compounds with larger HOMO–LUMO gaps amino *S*-**3b**, are nearly more electrophilicity (likely to involve reactions with a nucleophile) than *S*-**3a** (Table 2).

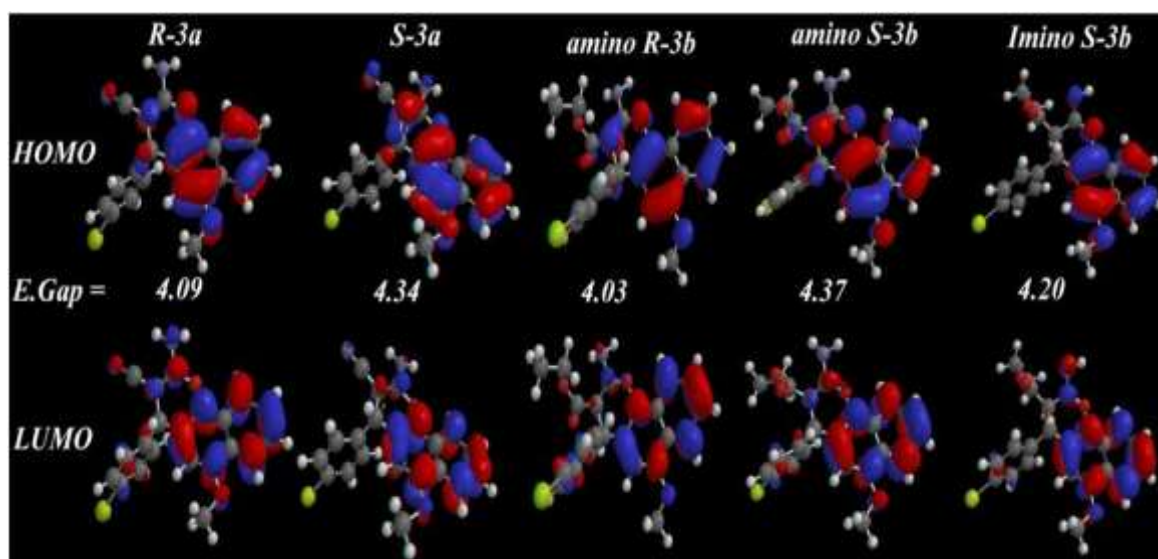


Fig. 3. The calculated HOMO, LUMO and HOMO-LUMO gap as calculated by AM1 semi-empirical with DFT B3LYP /6-311G*.

The total dipole moment is considering important physical quantity, it reflects the ability interaction of the molecules with the surrounding environment, *S*-enantiomer have a high dipole moments value (~ 4.93 and 3.28 Debye) than *R* isomer form (~ 4.48 and 3.20 Debye) for **3a** and amino **3b**, respectively, which increases its ability of interaction with the surrounding environments, and increase ability to binding with protein receptors, which increasing biological effects.

Flexible Alignment and Electrostatic potentials (ESP) mapped.

To gain clear vision of the similarity between the three dimensional structures of most stable compounds of *S*-**3a** and amino *S*-**3b** (*S* Figure 2 in supplementary material), a flexible alignment was employed using MOE [66] and exhibited a common features:

- (i) Comply of the benzo[*h*]chromene and methoxy phenyl rings.
- (ii) The superposition CO moiety of the ester fragment of amino *S*-**3b** compared with cyano moiety *S*-**3a** have a slight deviation distance (0.79 Å).
- (iii) The cyano group arranged in plane with benzo[*h*]chromene ring of *S*-**3a**, while in *S*-**3b**

the ester group occupy out of plane from the benzo[*h*]chromene ring with deviation angle (114°).

The electrostatic potentials mapped (ESP) was drawn, it represents a balance between repulsive interactions of the nuclei (positively-charged) and attractive interactions for the electrons (negatively-charged). The colors toward red depict negative potential (high electron density area, representing a strong attraction between the proton and the points on the molecular surface), while colors toward blue depict positive potential, and colors in between (orange, yellow, green) depict intermediate values of the potential. The ESP for compound **3a**, show nearly electronic similarity of two enantiomer structures, except, the negative potential is larger in amino group for *R*-form than *S*-form (Figure 4). The most negative potential area located in acetate moiety in **3b**, arranged by amino *S*-**3b** ≤ amino *R*-**3b** < imino *S*-**3b**, in contrary, the highest positive potential region included NH₂ group for amino *S*-**3b** compared with other compounds under investigation (Fig. 4).

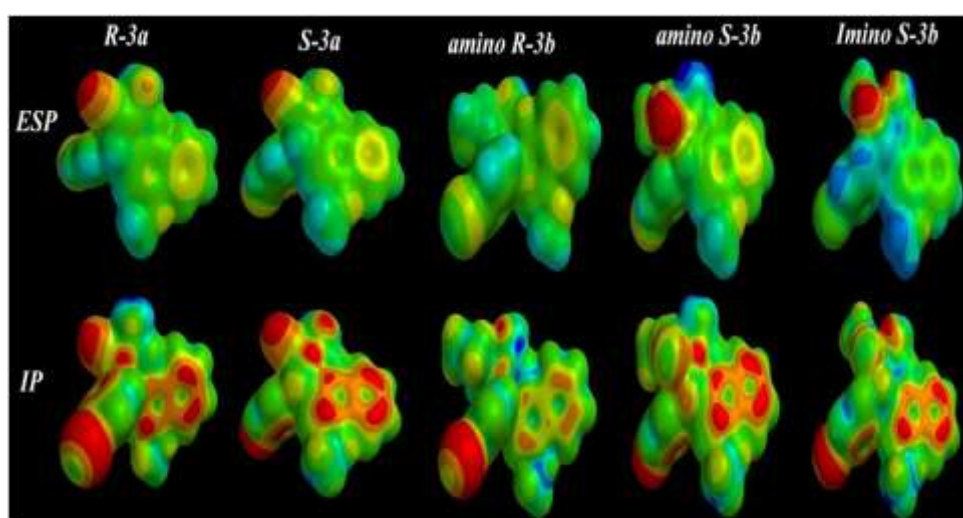


Fig. 4. The ESP and IP surfaces for **3a** and **3b** with AM1 with semi-empirical based on DFT-B3LYP/6-311G* calculations.

Charges and Ionization potential map (IP).

The Mulliken $q(M)$, electrostatic $q(el)$ and natural charges $q(n)$, were computed within full Bond Orbital analysis at AM1 semiempirical with B3LYP/6-311G* for the most stable compound **S-3a** and amino **S-3b** are shown in (S Table 3 in Supplementary material). The charge distributions over the atoms suggest that, the formation of donor and acceptor pairs involving the charge transfer in the molecule. In general in both compounds, the hydrogen atoms and some carbon atoms are positively charged, the O, N and Br atoms have negative charges, the nitrogen and bromine atoms in the molecules accepted the electrons. Replacement cyano group (**3a**) with ester group (**3b**) leads to a redistribution of electron density of molecule (S Table 5 in Supplementary material). The most negative centers in **S-3a** and amino **S-3b** involved in $-NH_2$, on the other hand the most positive charge are located on the C_1 in **S-3a** and amino **S-3b**, the maximum positive charge on the C_1 atom are due to attachment of the electronegative oxygen atom (withdrawing nature).

The local ionization potential (IP) was draw, it indicates the proportional electron removal facility around the molecule (ionization) [71,72] and measure the sensitivity of a molecular zone toward electrophilic attack (reactivity). The default program value (Fixed Value: (0.032e); Medium Resolution), is used for the surface mapped values of the (IP) (Figure 4). The red color representing a region with highest likely attack with electrophile, and the blue regions likely attack with nucleophile (lowest electrophilic regions). The examination structures in (Figure 4) shows that, the **S**-enantiomer has more electron rich around the surface of the molecule than of **R**-enantiomer for **3a** and **3b**, and amino form is electron richer than imino tautomer structure for **S-3b**. This data suggest,

the **S**-enantiomer form for **3a** and amino **3b** are undergoing reaction, and occurring with higher conformation energy than **R**-forms, and the examination of the distribution ideal charge for IP surface exhibits, the electrophile attack on surface of two enantiomer is favorable at **S**-Form, which given the red-yellow color distribution.

Global and local reactivity descriptors:

Density functional theory has been successful to recognize the chemical reactivity and site selectivity of the molecular systems, several global and local chemical reactivity descriptors for molecules have been defined, like S ; softness (measures stability of molecules and chemical reactivity with direct proportional) [73] η ; hardness (reciprocal of softness), μ ; chemical potential, χ ; electronegativity (strength atom for attracting electrons to itself), ω ; electrophilicity index (measuring lowering energy due to maximal flowing electron between donor and acceptor), the Fukui function and the philicity [73-78]

$$\eta = \frac{1}{2} \left(\frac{\partial^2 E}{\partial^2 N^2} \right)_{V(f)} = \frac{1}{2} \left(\frac{\partial \mu}{\partial N^2} \right)_{V(f)} \quad (1)$$

$$\mu = \left[\frac{\partial E}{\partial N} \right]_{V(f)} \quad (2)$$

$$\chi = -\mu = - \left[\frac{\partial E}{\partial N} \right]_{V(f)} \quad (3)$$

$$S = \frac{1}{\eta} \quad (4)$$

$$\omega = \frac{\mu^2}{2\eta} \quad (5)$$

Where E is electronic energy, and $V(r)$ are and external potential of an N -electron system.

The amino **S-3b** has smallest hardness value, which indicating its more reactive molecule (Table 4), this behavior may be explained by a large bond order for carbonyl group, exhibiting a stronger electron-attractor effect, that might be related with a localization of electronic density on its atom (Figure 4).

The electrophilicity index values indicate that, the global electrophilic capacity of **S-** larger than **R-** form for **3a** and **3b**, and amino **S-3b** more than imino **S-3b**, which leading to increasing susceptibly of nucleophilic attack on this molecule.

ADMET factors profiling:

Oral bioavailability was considered playing an important role for the development of bioactive molecules as therapeutic agents. Many potential therapeutic agents fail to reach the clinic, because of their ADMET (absorption, distribution, metabolism, elimination and toxic) factors. Therefore, a computational study for prediction of ADMET properties of the molecules was performed for compounds **3a** and **3b**, by the determination of topological polar surface area (TPSA), a calculated percent absorption (% ABS) which was estimated by Zhao *et al.* equation [79] and “rule of five” formulated by Lipinski [80] which established that, chemical compound could be an orally active drug in humans, if no more than one violation of the following rule:

- (i) ClogP (partition coefficient between water and octanol) < 5 .
- (ii) Number of hydrogen bond donors sites ≤ 5 .
- (iii) Number of hydrogen bond acceptors sites ≤ 10 .

(iv) Molecular weight < 500 and molar refractivity should be between 40-130. In addition, the total polar surface area (TPSA) is another key property linked to drug bioavailability, the passively absorbed molecules with (TPSA >140) have low oral bioavailability [81].

All calculated descriptors were performed using MOE Package [5], and their results were disclosed in (Table 5). Our results revealed that, the CLogP (factor of the lipophilicity [82] was less than 5.0 except **S-3b**, the molecular weight (MW < 500), hydrogen bond acceptors (4), hydrogen bond donors (1) and molar refractivity values ranged (~ 113 -124), this data show these compounds fulfill Lipinski’s rule. Also, the percent absorption of **R-** enantiomer less than **S-** enantiomer for **S-3b**.

The drug-likeness calculated (Table 6), according to (ADME-T) algorithm [83-84]. It was examined the ability of compounds for transported across the intestinal epithelium, they probably have high affinity binding to the plasma proteins, and may be through the blood-brain barrier, and it necessary for ability drug transported throughout the body. In general, No marked health effects in rodent toxicity profiles were observed among its compounds **S-3a** and amino **S-3b**. From these data one can suggest that, the compounds can be used as a good oral absorption.

REFERENCES:

- 1) A.M. El-Agrody, M.H. El-Hakium, M.S. Abd El-Latif, A.H. Fekry, E.S.M. El-Sayed, K.A. El-Gareab, *Acta Pharm.*, (2000) , **50**, 111.
- 2) M.C. Yimdjo, A.G. Azebaze, A.E. Nkengfack, A. Michele Meyer, B. Bodo, Z.T. Fomum, *Phytochemistry*, (2004), **65**, 2789.

- 3) Ze-Qi Xu, Krzysztof Papek, W.J. Suling, L. Enache, M.T. Flavin, *Bioorg. Med. Chem. Lett.*, 14 (2006) 4610.
- 4) V. Jeso, K.C. Nicolaou, *Tetrahedron Lett.*, (2009), **50**, 1161.
- 5) L. Alvey, S. Prado, B. Saint-Joanis, S. Michel, M. Koch, S.T. Cole, F. Tillequin, Y.L. Janin, *Eur. J. Med. Chem.*, (2009) **44**, 2497.
- 6) L. Alvey, S. Prado, V. Huteau, B. Saint-Joanis, S. Michel, M. Koch, S.T. Cole, F. Tillequin, Y.L. Janin, *Bioorg. Med. Chem.*, (2008) **16**, 8264.
- 7) T. Symeonidis, M. Chamilos, D.J. Hadjipavlou-Litina, M. Kallitsakis, K.E. Litinas, *Bioorg. Med. Chem. Lett.*, (2009), **19**, 1139.
- 8) T. Narender, Shweta, S. Gupta, *Bioorg. Med. Chem. Lett.*, (2009), **14**, 3913.
- 9) D. B. daSilva, E. C. O. Tulli, G. C. G. Militao, L.V. Costa-Lotufu, C. Pessoa, M. O. De Moraes, S. Albuquerque, J. M. deSiqueira, *Phytomedicine*, (2009), 70, 590.
- 10) J. C. A. Tanaka, C. C. da Silva, I. C. P. Ferreira, G. M. C. Machado, L. L. Leon, A. J. B. de Oliveira, *Phytomedicine*, (2007), **14**, 377.
- 11) V. Lakshmi, K. Pandey, A. Kapil, N. Singh, M. Samant, A. Dube, *Phytomedicine*, 1 (2007) **4**, 36.
- 12) E. C. Torres-Santos, D. Lopes, R. Rodrigues Oliveira, J. P. P. Carauta, C. A. Bandeira Falcao, M. A. C. Kaplan, B. Rossi-Bergmann, *Phytomedicine*, (2004), **11**, 114.
- 13) A. Rampa, A. Bisi, F. Belluti, S. Gobbi, L. Piazzini, P. Valenti, A. Zampiron, A. Caputo, K. Varani, P.A. Borea, M. Carrara, *IL Farmaco*, (2005), **60**, 135.
- 14) Quan-Bin Han, Nian-Yun Yang, Hong-Lei Tian, Chun-Feng Qiao, Jing-Zheng Song, Donald C. Chang, Shi-Lin Chen, Kathy Q. Luo, Hong-Xi Xu, *Phytochemistry*, (2008), **69**, 2187.
- 15) W. Kemnitzer, J. Drewe, S. Jiang, H. Zhang, C. Crogan-Grundy, D. Labreque, M. bubenick, G. Attardo, R. Denis, S. Lamothe, H. Gourdeau, B. Tseng, S. Kasibhatla, S. Xiong Cai, *J. Med. Chem.*, (2008), **51**, 417.
- 16) V.K. Tandon, M. Vaish, S. Jain, D.S. Bhakuni, R.C. Srimal, *Indian J. Pharm. Sci.*, (1991), **53**, 22.
- 17) M. Brunavs, C.P. Dell, P.T. Gallagher, W.M. Owton and C.M. Smith, *European Pat. Appl. EP.* (1993), **557**, 075; *Chem. Abstr.*, (1994), **120**, 106768t.
- 18) V. Magedov, M. Manpadi, M.A. Ogasawara, A.S. Dhawan, S. Rogelj, S. van Slambrouk, W.F.A. Steelant, N.M. Evdokimov, P.Y. Uglinskii, E.M. Elias, E.J. Knee, P. Tongwa, M. Yu. Antipin, A. Kornienko, *J. Med. Chem.*, (2008), **51**, 2561.
- 19) F. Eiden, F. Denk, *Arch. Pharm. Weinheim Ger.*, (1991), **324**, 875.
- 20) C. Bruhlmann, F. Ooms, P. Carrupt, B. Testa, M. Catto, F. Leonetti, C. Altomare, A. Cartti, *J. Med. Chem.*, (2001), **44**, 3195.
- 21) S.R. Kesten, T.G. Heffner, S.J. Johnson, T.A. Pugsley, J.L. Wright, D.L. Wise, *J. Med. Chem.*, (1999), **42**, 3718.
- 22) W.P. Smith, L.S. Sollis, D.P. Howes, C.P. Cherry, D.I. Starkey, N.K. Cobley, *J. Med. Chem.*, (1998), **41**, 787.
- 23) R.N. Taylor, A. Cleasby, O. Singh, T. Sharzynski, J.A. Wonacott, W.P. Smith, L.S. Sollis, D.P. Howes, C.P. Cherry, R. Bethell, P. Colman, J. Varghese, *J. Med. Chem.*, (1998), **41**, 798.
- 24) J.-F. Cheng, A. Ishikawa, Y. Ono, T. Arrhenius, A. Nadzan, *Bioorg. Med. Chem. Lett.*, 13 (2003) 3647.
- 25) V.P. Sharma, *Asian J. Chem.*, (2004), **16**, 1966; *Chem. Abstr.*, 142, 298061
- 26) V.P. Sharma, *Indian J. Heterocycl. Chem.*, (2004), **14**, 35; *Chem. Abstr.*, 142, 373785.

- 27) P. Gebhardt, K. Dornberger, F.A. Gollmick, U. Gräfe, A. Härtl, H. Görls, B. Schlegel, C. Hertweck *Bioorg. Med. Chem. Lett.*, (2007), **17**, 2558.
- 28) G. Melagraki, A. Afantitis, O. Igglessi-Markopoulou, A. Detsi, M. Koufaki, C. Kontogiorgis, Di. J. Hadjipavlou-Litina, *Eur. J. Med. Chem.*, (2009), **44**, 3020.
- 29) T. Symeonidis, K.C. Fylaktakidou, D.J. Hadjipavlou-Litina and K.E. Litinas, *Eur. J. Med. Chem.*, (2009), **44**, 5012.
- 30) S. Begum, B. Saxena, Ma. Goyal, R. Ranjan, V.B. Joshi, C. V. Rao, S. Krishnamurthy, M. Sahai, *Fitoterapia*, (2010), **81**, 178.
- 31) J.J. Anil, R.A. Kumar, S.A. Rasheed, S.P. Chandrika, A. Chandrasekhar, S. Baby, A. Subramoniam, *J. Ethnopharm.*, (2010), **130**, 267.
- 32) K. Hiramoto, A. Nasuhara, K. Michiloshi, T. Kato and K. Kikugawa, *Mutat. Res.*, (1997), **395**, 47.
- 33) A.G. Martinez and L.J. Marco, *Bioorg. Med. Chem. Lett.*, (1997), **7**, 3165.
- 34) W.O. Foye, *Principi Di Chimica Farmaceutica; Piccin: Padova, Italy*, (1991) **416**.
- 35) L. Bonsignore, G. Loy, D. Secci, A. Calignano, *Eur. J. Med. Chem.*, (1993), **28**, 517.
- 36) A. Gajbhiye, V. Mallareddy and G. Achaiiah, *Indian J Pharm Sci.*, (2008), **70**, 118.
- 37) M. Ghate, R.A. Kusanur and M.V. Kulkarni, *Eur. J. Med. Chem.*, (2005), **40**, 882.
- 38) T. El-Sayed Ali and M.A. Ibrahim, *J. Braz. Chem. Soc.*, 21 (2010) 1007.
- 39) B. Narasimhan, P. Kumar, D. Sharma, *Acta Pharm. Sci.*, 52 (2010) 169.
- 40) K.M. Amin, M.M. Kamel, M.M. Anwar, M. Khedr and Y.M. Syam, *Eur. J. Med. Chem.*, (2010), **45**, 2117.
- 41) R.S. Keri, K.M. Hosamani, R.V. Shingalapur and M.H. Hugar, *Eur. J. Med. Chem.*, (2010), **45**, 2597.
- 42) G. Bianchi and A. Tava, *Agric. Biol. Chem.*, (1987), **51**, 2001.
- 43) A. M. El-Agrody, *J. Chem. Res. (S)* (1994) 280.
- 44) A.M. El-Agrody, H. A. Emam, M.H. El-Hakim, M. S. Abd El-Latif, A. H. Fakery, *J. Chem. Res. (S)* (1997) 320.
- 45) A. M. El-Agrody, H. A. Emam, M. H. El-Hakim, M. S. Abd El-Latif, A. H. Fakery, *J. Chem. Res. (M)* (1997) 2039.
- 46) H. Bedair, N. A. El-Hady, M. S. Abd El-Latif, A. H. Fakery, A. M. El-Agrody, *IL Farmaco*, (2000), **55**, 708.
- 47) M. El-Agrody, M. H. El-Hakim, M. S. Abd El-Latif, A. H. Fakery, E. S. M. El-Sayed, K. A. El-Ghareab, *Acta Pharm.*, 50 (2000) 111.
- 48) Z. Sayed, N. A. El-Hady and A. M. El-Agrody, *J. Chem. Res. (S)* (2000) 146.
- 49) M. El-Agrody, M. S. Abd El-Latif, N. A. El-Hady, A. H. Fakery, A. H. Bedair, *Molecules*, (2000), **6**, 519.
- 50) H. Bedair, H. A. Emam, N. A. El-Hady, K. A. R. Ahmed and A. M. El-Agrody, *IL Farmaco*, (2001), **56**, 965.
- 51) M. El-Agrody, F. A. Eid, H. A. Emam, H. M. Mohamed and A. H. Bedair, *Z. Naturforsch., Teil B*, (2002), **57**, 579.
- 52) M. M. Khafagy, A. H. F. Abd El-Wahab, F. A. Eid and A. M. El-Agrody, *IL Farmaco*, (2002), **57**, 715.
- 53) F. A. Eid, A. H. Bedair, H. A. Emam, H. M. Mohamed and A. M. El-Agrody, *Al-Azhar Bull. Sci.*, (2003), **14**, 311.
- 54) A. S. Abd-El-Aziz, A. M. El-Agrody, A. H. Bedair, T. Christopher Corkery and A. Ata, *Heterocycles*, (2004), **63**, 1793.
- 55) S. Abd-El-Aziz, H. M. Mohamed, S. Mohammed, S. Zahid, A. Ata, A. H. Bedair, A. M. El-Agrody and P. D. Harvey, *J. Heterocycl. Chem.*, (2007), **44**, 1287.

- 56) N. M. Sabry , H. M. Mohamed, Essam Shawky A. E. H. Khattab , S. S. Motlaq , A. M. El-Agrody, *Eur. J. Med. Chem.*, (2011) ,**46** ,765.
- 57) A. M. El-Agrody, N.M. Sabry and S.S. Motlaq, *J. Chem. Res.*, (2011),**35** 77.
- 58) Spartan 08, Wave function Inc., Irvine, CA 92612, USA, 2008.
- 59) P. Hohenberg and W. Kohn, *Phys. Rev. B*(1964) ,**136** ,864.
- 60) W. Kohn and L.J. Sham, *Phys. Rev. A* (1965), **140**, 1133.
- 61) W.J. Hehre, L. Radom, P.V.R. Schleyer, J.A. Pople, *Ab Initio Molecular Orbital Theory*. John Wiley & Sons, New York, (1986).
- 62) J. Sauer, *Chem. Rev.* (1989), **89** ,199-255.
- 63) J.J.P. Stewart, *J. Comput. Chem.* (1989) ,**10** ,209.
- 64) U.C. Singh, P.A. Kollman, An approach to computing electrostatic charges for molecules, *J. Comput. Chem.* (1984), **5** , 129–145.
- 65) M.L. Connolly, Solvent-accessible surfaces of proteins and nucleic acids, *Science* (1983) ,**221** ,709–713.
- 66) S. Sagdinc, B. Koksoy, F. Kandemirli, S.H. Bayari, *J. Mol. Struct.* 63 (2009) 917.
- 67) A. Rauk, *Orbital Interaction Theory of Organic Chemistry*, 2nd ed., Wiley Interscience, New York, (2001), pp. 86–136.
- 68) A. Streitwieser Jr., *Molecular Orbital Theory for Organic Chemists*, Wiley New York, 1961.
- 69) I.Fleming,. (*Frontier Orbitals and Organic Chemical Reactions*), John Wiley and Sons, Academic Press, New York 1976.
- 70) Chemical Computing Group. Inc, MOE, 2009, 10.
- 71) P. Sjoberg, J.S. Murray, T. Brinck, P. Politzer, *Can. J. Chem.* (1990) , **68** ,1440.
- 72) P. Politzer, J.S. Murray, M.C. Concha, *Int. J. Quant. Chem.* (2002) ,**88** ,19.
- 73) Parr, R. G.; Chattaraj, P. K. *J. Am. Chem. Soc.* (1991), **113**, 1854.
- 74) Parr, R. G.; Szentpaly, L. V.; Liu, S. J. *Am. Chem. Soc.* (1999), **121**, 1922.
- 75) Chattaraj, P. K.; Maiti, B.; Sarkar, U. J. *Phys. Chem. A*, (2003), **107**, 4973.
- 76) Parr, R. G.; Donnelly, R. A.; Levy, M.; Palke, W. E. *J. Chem. Phys.* (1978), **68**, 801.
- 77) Parr, R. G.; Pearson, R. G. *J. Am. Chem. Soc.* (1983),**105**, 7512.
- 78) Parr, R. G.; Yang, W. *Density Functional Theory of Atoms and Molecules*; Oxford University Press: Oxford, UK, 1989.
- 79) Zhao, Y.; Abraham, M.H.; Lee, J.; Hersey, A.; Luscombe, N.Ch.; Beck, G.; Sherborne, B.; Cooper, I.; *Pharm. Res.* (2002), **19**, 1446.
- 80) Lipinski, C.A.; Lombardo, F.; Dominy, B.W.; Feeney, P.J.; *Adv. Drug. Delivery Rev.* (1997),**23**, 3.
- 81) Clark, D.E.; Pickett, S.D.; *Drug Discov. Today*, (2000), **5**, 49.
- 82) Wildman, S.A.; Crippen, G.M., *J. Chem. Inf. Comput. Sci.* (1999), **39** , 868.
- 83) *Pharma Algorithms (Web Edition)* (2009),**5**.
- 84) T.L. Moda, L.G. Torres, A.E. Carrara, A.D. Andricopulo, PK/DB: database for pharmacokinetic properties and predictive in silico ADME models. *Bioinformatics* (2008), **24**, 2270.

TABLES:

Table 1: The Optimized Calculations Energies and thermodynamic parameters of **3a** and **3b** at AM1 Semi-empirical using DFT/B3LYP with 6-311G* basis sets.

CPD	E	Eaq	ZPE	S°	C _v °	H°	G°
R-3a	-2286070.75	-2286081.00	945.09	562.16	342.78	-3593.69052	-3539.75248
S-3a	-2286377.54	-2286387.97	847.80	545.56	318.44	-4303.74602	-3665.36415
amino R-3b	-2316705.86	-2316714.69	1155.64	587.07	360.77	-3691.41831	-3691.48450
amino S-3b	-2348968.21	-2348977.75	1150.74	578.44	353.00	-3691.44253	-3691.50919
iminoS-3b	-2331496.04	-2331505.09	1157.62	582.85	360.46	-3691.44231	-3691.50800

E: The total energy (kcal/mol)., **Eaq:** aqueous energy (kcal/mol) (heat of formation + strain energy), **ZPE:** zero-point vibrational energies(kj/mol), **S°:** Entropy (kj/mol), **C_v°:** Constant volume molar heat capacity, **H°:** Enthalpy (kj/mol), **G°:** Gibbs free energy (kj/mol).

Table 2: Optimized geometrical parameters of **S-3a** at AM1 Semi-empirical using DFT/B3LYP with 6-31G* and 6-311G* basis sets.

BOND LENGTH			BOND ANGLE					
Atom Number	6311 G*	631 G*	Atom Number	6311 G*	631 G*	Atom Number	6311 G*	631 G*
C(1)-N(26)	1.3773	1.3685	C(19)-C(24)-C(23)	120.6468	121.2661	C(14)-C(7)-C(8)	118.3384	119.0895
C(3)-C(19)	1.5310	1.5331	C(24)-C(23)-C(22)	119.7725	118.8748	C(14)-C(7)-C(6)	122.1816	121.9934
C(22)-Br(25)	1.8901	1.9168	Br(25)-C(22)-C(23)	119.7689	119.6383	C(8)-C(7)-C(6)	119.4799	118.8628
C(19)-C(24)	1.4064	1.3974	Br(25)-C(22)-C(21)	119.7671	119.2444	O(17)-C(6)-C(7)	116.1485	114.9804
C(23)-C(24)	1.3966	1.3975	C(23)-C(22)-C(21)	120.4640	119.0895	O(17)-C(6)-C(5)	123.7675	124.6737
C(22)-C(23)	1.3925	1.3917	C(22)-C(21)-C(20)	119.8137	121.1209	C(7)-C(6)-C(5)	120.0837	120.3451
C(21)-C(22)	1.3928	1.3957	C(21)-C(20)-C(19)	120.6101	120.4785	C(9)-C(4)-C(5)	119.2410	121.2907
C(20)-C(21)	1.3969	1.3924	C(3)-C(19)-C(24)	121.3584	120.9837	C(9)-C(4)-C(3)	120.1308	118.7808
C(19)-C(20)	1.4054	1.4006	C(3)-C(19)-C(20)	119.9417	118.5311	C(5)-C(4)-C(3)	120.6245	122.0349
C(6)-O(17)	1.3751	1.3622	C(24)-C(19)-C(20)	118.6898	118.2635	C(19)-C(3)-C(4)	112.1333	119.1811
O(17)-C(18)	1.4216	1.4199	C(19)-C(24)-C(23)	120.6468	178.6495	C(19)-C(3)-C(2)	111.5320	111.9752
C(2)-C(15)	1.4254	1.4166	C(24)-C(23)-C(22)	119.7725	120.6013	C(19)-C(3)-H(27)	108.4442	111.9964
C(15)-N(16)	1.1603	1.1679	Br(25)-C(22)-C(23)	119.7689	120.264	C(4)-C(3)-C(2)	112.5965	109.8364
C(8)-C(11)	1.4134	1.4180	Br(25)-C(22)-C(21)	119.7671	120.4496	C(4)-C(3)-H(27)	105.0904	107.8007
C(7)-C(14)	1.4134	1.4161	C(6)-O(17)-C(18)	117.8843	120.5083	C(2)-C(3)-H(27)	106.5945	108.618
C(13)-C(14)	1.3951	1.3789	C(2)-C(15)-N(16)	179.5461	118.9506	C(15)-C(2)-C(3)	117.5558	119.4951
C(12)-C(13)	1.3867	1.4122	C(7)-C(14)-C(13)	121.8336	122.6719	C(15)-C(2)-C(1)	120.9517	117.9126
C(11)-C(12)	1.3948	1.3786	C(14)-C(13)-C(12)	119.7190	114.9498	C(3)-C(2)-C(1)	121.4644	122.5904
C(1)-O(10)	1.3873	1.3522	C(13)-C(12)-C(11)	119.6952	122.3764	N(26)-C(1)-O(10)	112.4814	110.7969
C(9)-O(10)	1.3791	1.3930	C(8)-C(11)-C(12)	121.6348	122.6244	N(26)-C(1)-C(2)	125.3973	125.8135
C(4)-C(9)	1.3961	1.3718	C(1)-O(10)-C(9)	120.4756	119.0327	O(10)-C(1)-C(2)	122.1181	123.3457
C(8)-C(9)	1.4136	1.4260	O(10)-C(9)-C(4)	121.2415	118.3428			
C(7)-C(8)	1.4179	1.4280	O(10)-C(9)-C(8)	117.4350	119.1438			
C(6)-C(7)	1.4178	1.4350	C(4)-C(9)-C(8)	121.3216	121.2661			
C(5)-C(6)	1.3980	1.3765	C(11)-C(8)-C(9)	122.1854	118.8748			
C(4)-C(5)	1.4030	1.4221	C(11)-C(8)-C(7)	118.7788	119.6383			
C(3)-C(4)	1.5161	1.5199	C(9)-C(8)-C(7)	119.0355	119.2444			

Table 3 Optimized geometrical parameters of amino **S-3b** at Semi-empirical AM1 and DFT\B3LYP with 6- 31G* and 6-311G* basis sets:

Atom Number	BOND LENGTH		BOND ANGLE			BOND ANGLE		
	6311 G*	631 G*	Atom Number	6311 G*	631 G*	Atom Number	6311 G*	631 G*
C(28)-C(29)	1.5140	1.5170	C(29)-C(28)-O(2)	107.7768	107.7768	C(12)-C(7)-C(6)	120.2698	121.6434
O(2)-C(28)	1.3890	1.4426	C(20)-C(25)-C(24)	120.6947	123.5347	C(8)-C(7)-C(6)	120.4773	120.3617
C(1)-C(5)	1.5170	1.4703	C(25)-C(24)-C(23)	119.7723	117.8861	C(20)-C(6)-C(7)	112.6494	118.3297
C(4)-N(27)	1.4620	1.3769	Br(26)-C(23)-C(24)	119.7758	119.7708	C(20)-C(6)-C(5)	111.3515	122.1655
C(6)-C(20)	1.4970	1.5319	Br(26)-C(23)-C(22)	119.7514	118.9846	C(20)-C(6)-H(30)	108.2166	119.5048
C(23)-Br(26)	1.8810	1.8900	C(24)-C(23)-C(22)	120.4722	121.2444	C(7)-C(6)-C(5)	111.9736	122.1803
C(20)-C(25)	1.4200	1.4057	C(23)-C(22)-C(21)	119.7806	119.7723	C(7)-C(6)-H(30)	104.7226	118.774
C(24)-C(25)	1.4200	1.3966	C(22)-C(21)-C(20)	120.6630	119.7758	C(5)-C(6)-H(30)	107.5071	119.0456
C(23)-C(24)	1.4200	1.3925	C(6)-C(20)-C(25)	119.5871	119.7514	C(1)-C(5)-C(6)	114.9043	117.3203
C(22)-C(23)	1.4200	1.3924	C(6)-C(20)-C(21)	121.7568	120.4722	C(1)-C(5)-C(4)	121.9802	121.414
C(21)-C(22)	1.4200	1.3968	C(25)-C(20)-C(21)	118.6140	119.7806	C(6)-C(5)-C(4)	122.7918	121.2656
C(20)-C(21)	1.4200	1.4064	C(9)-O(18)-C(19)	117.8861	120.6947	N(27)-C(4)-O(13)	112.5567	119.2499
C(9)-O(18)	1.3550	1.3753	C(10)-C(17)-C(16)	121.8442	120.663	N(27)-C(4)-C(5)	125.9596	120.2698
O(18)-C(19)	1.3960	1.4216	C(17)-C(16)-C(15)	119.7184	118.614	O(13)-C(4)-C(5)	121.4802	120.4773
C(11)-C(14)	1.4200	1.4136	C(16)-C(15)-C(14)	119.6902	119.5871	C(28)-O(2)-C(1)	123.5347	121.6434
C(10)-C(17)	1.4200	1.4135	C(11)-C(14)-C(15)	121.6434	121.7568	C(5)-C(1)-O(3)	119.7708	120.3617
C(16)-C(17)	1.4200	1.3952	C(4)-O(13)-C(12)	120.3617	122.7918	C(5)-C(1)-O(2)	118.9846	118.3297
C(15)-C(16)	1.4200	1.3867	O(13)-C(12)-C(7)	121.4140	114.9043	O(3)-C(1)-O(2)	121.2444	122.1655
C(14)-C(15)	1.4200	1.3948	O(13)-C(12)-C(11)	117.3203	121.9802			
C(4)-O(13)	1.3550	1.3881	C(7)-C(12)-C(11)	121.2656	112.5567			
C(12)-O(13)	1.3550	1.3803	C(14)-C(11)-C(12)	122.1803	125.9596			
C(7)-C(12)	1.4200	1.3975	C(14)-C(11)-C(10)	118.7740	121.4802			
C(11)-C(12)	1.4200	1.4138	C(12)-C(11)-C(10)	119.0456	119.7184			
C(10)-C(11)	1.4200	1.4180	C(17)-C(10)-C(11)	118.3297	119.6902			
C(9)-C(10)	1.4200	1.4178	C(17)-C(10)-C(9)	122.1655	121.8442			
C(8)-C(9)	1.4200	1.3979	C(11)-C(10)-C(9)	119.5048	116.135			
C(7)-C(8)	1.4200	1.4030	O(18)-C(9)-C(10)	116.1350	123.7806			
C(6)-C(7)	1.4970	1.5181	O(18)-C(9)-C(8)	123.7806	120.0844			
C(5)-C(6)	1.4970	1.5033	C(10)-C(9)-C(8)	120.0844	120.8411			
C(4)-C(5)	1.3370	1.3445	C(4)-O(13)-C(12)	120.3617	112.6494			
C(1)-O(3)	1.2080	1.2274	C(9)-C(8)-C(7)	120.8411	111.3515			
C(1)-O(2)	1.3380	1.3532	C(12)-C(7)-C(8)	119.2499	111.9736			

Table 4: The reactivity descriptors of **3a** and **3b** at AM1 Semi-empirical using DFT/B3LYP with 6-311G* basis set.

CPD	HOMO	LUMO	ΔG	η	S	χ	μ	ω	D
R-3a	-5.68	-1.59	4.09	2.045	0.488998	3.635	-3.635	3.230617	4.48
S-3a	-5.81	-1.67	4.14	2.07	0.483091	3.74	3.3786	-5.81	4.93
amino R-3b	-5.67	-1.67	4.00	2.00	0.500000	3.505	-3.670	3.367225	3.20
amino S-3b	-5.76	-1.73	4.03	2.015	0.496278	3.745	-3.745	3.480155	3.28
iminoS-3b	-5.69	-1.32	4.37	2.185	0.457666	3.67	-3.505	2.811219	3.41

HOMO: Highest Occupied Molecular Orbital (eV), **LUMO**: Lowest Occupied Molecular Orbital (eV), ΔG : difference between HOMO and LUMO energy levels(eV), η : *Hardness*(eV), **S**: Softness(eV), χ : Electronegativity (eV), μ : chemical potential (eV), ω : Electrophilicity (eV), **D**: dipole moment (Deby).

Table 5: Pharmacokinetic parameters important for good oral bioavailability of compounds **3a** and **3b**:

CPD	Area	PSA	%ABS	Vol.	P	Logp	HBD	HBA	V	mr	Log S
2R	367.14	51.541	91.218	355.97	69.28	4.81	1	4	0	113.62	-7.30
2S	336.10	50.681	91.515	355.22	69.16	4.81	1	4	0	113.62	-7.30
3R NH2	407.80	50.873	91.448	394.47	70.67	5.50	1	4	1	124.16	-7.66
3S NH2	407.00	50.418	91.605	393.67	70.85	5.50	1	4	1	124.16	-7.66
3S-imino	400.04	45.678	93.241	392.72	70.52	6.08	0	0	1	123.92	-7.68

PSA A⁰²: Polar surface area, *%ABS*: Absorption percentage, *Vol*: Volume (A³), *P*: polarizability
Log P: Calculated lipophilicity., *Log S*: Solubility parameter, *HBA*: Number of hydrogen bond acceptor, *HBD*: Number of hydrogen bond donor, *V*: Number of violation from Lipinski's rule of five., *mr*: Molar Refractivity

Table 6: The predicted ADME-Tox of the compound **S-3a** and amino **S-3b**.

ADME-Tox	S-3a	S-3b
LogBBB (Blood-brain barrier.)	0.030	0.018
PPB% (Plasma protein binding)	98.79%	98.33
LD50 rat/mouse(mg kg ⁻¹ , oral)	100/240	500/590
LD50 rat/mouse(mg kg ⁻¹ , intraperitoneal)	280/360	310/360
LD50 mouse(mg kg ⁻¹ , intravenous)	46	38
LD50 mouse(mg kg ⁻¹ , subcutaneous)	70	220
Ames test (genotoxicity, %)	0.65	0.66
Prob. of blood effect	0.83	0.55
Prob. of cardiovascular System	0.95	0.96
Prob. of gastrointestinal System	0.9	0.96
Prob. of kidney effect	0.95	0.82
Prob. of liver effect	0.46	0.24
Prob. of lung effect	0.67	0.91

Sup. Table 1: Optimized geometrical parameters of **R-3a**, amino **R-3b** and Imino **S-3b** at Semi-empirical AM1 and DFT-B3LYP with 6-311G** basis set:

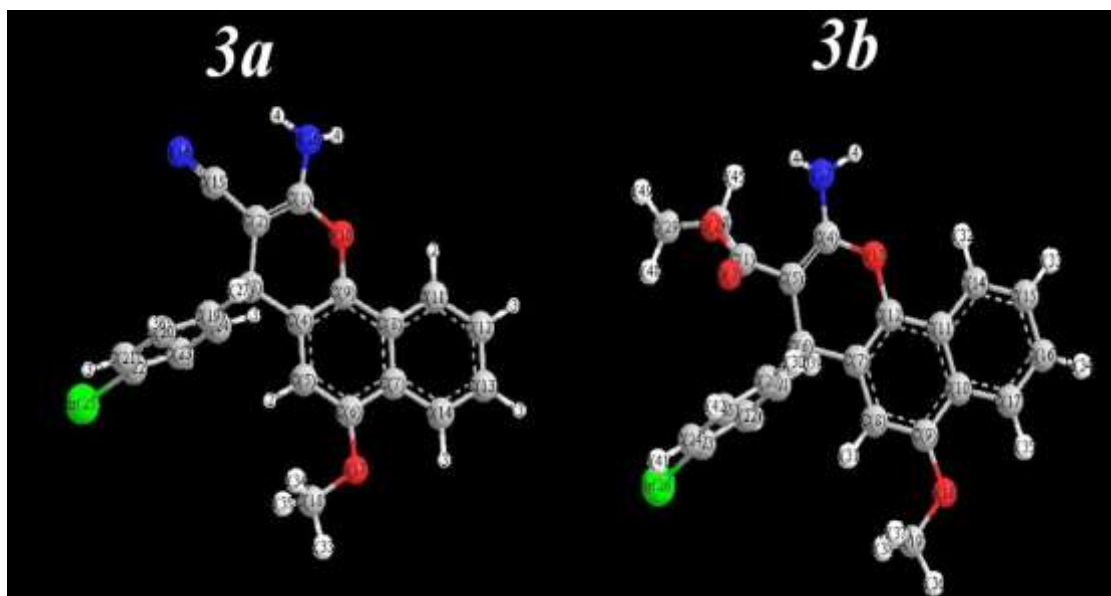
R-3a						amino R-3b		Imino S-3b
Atom Number	Length	Atom Number	angle	Atom Number	angle	Atom Number	Length	Length
C(22)-Br(25)	1.9168	C(24)-C(23)-C(22)	118.8748	C(7)-C(6)-C(5)	120.3451	C(28)-C(29)	1.5170	1.5182
C(19)-C(24)	1.3974	Br(25)-C(22)-C(23)	119.6383	C(6)-C(5)-C(4)	121.2907	O(2)-C(28)	1.4426	1.4433
C(23)-C(24)	1.3975	Br(25)-C(22)-C(21)	119.2444	C(9)-C(4)-C(5)	118.7808	C(1)-C(5)	1.4703	1.5425
C(22)-C(23)	1.3917	C(23)-C(22)-C(21)	121.1171	C(9)-C(4)-C(3)	122.0349	C(4)-N(27)	1.3769	1.2682
C(21)-C(22)	1.3957	C(24)-C(23)-C(22)	118.8748	C(5)-C(4)-C(3)	119.1811	C(6)-C(20)	1.5319	1.5240
C(20)-C(21)	1.3924	Br(25)-C(22)-C(23)	119.6383	C(19)-C(3)-C(4)	111.9752	C(23)-Br(26)	1.8900	1.9189
C(19)-C(20)	1.4006	Br(25)-C(22)-C(21)	119.2444	C(19)-C(3)-C(2)	111.9964	C(20)-C(25)	1.4057	1.3992
C(6)-O(17)	1.3622	C(23)-C(22)-C(21)	121.1171	C(4)-C(3)-C(2)	109.8364	C(24)-C(25)	1.3966	1.3963
O(17)-C(18)	1.4199	C(24)-C(23)-C(22)	118.8748	C(4)-C(3)-H(27)	107.8007	C(23)-C(24)	1.3925	1.3924
C(2)-C(15)	1.4166	Br(25)-C(22)-C(23)	119.6383	C(2)-C(3)-H(27)	108.6180	C(22)-C(23)	1.3924	1.3942
C(15)-N(16)	1.1679	Br(25)-C(22)-C(21)	119.2444	C(15)-C(2)-C(3)	119.4951	C(21)-C(22)	1.3968	1.3942
C(8)-C(11)	1.4180	C(23)-C(22)-C(21)	121.1171	C(15)-C(2)-C(1)	117.9126	C(20)-C(21)	1.4064	1.4027
C(7)-C(14)	1.4161	C(3)-C(19)-C(24)	120.4785	C(3)-C(2)-C(1)	122.5904	C(9)-O(18)	1.3753	1.3637
C(13)-C(14)	1.3789	C(3)-C(19)-C(20)	120.9837	N(26)-C(1)-O(10)	110.7969	O(18)-C(19)	1.4216	1.4195
C(12)-C(13)	1.4122	C(24)-C(19)-C(20)	118.5311	N(26)-C(1)-C(2)	125.8135	C(11)-C(14)	1.4136	1.4185
C(11)-C(12)	1.3786	C(6)-O(17)-C(18)	118.2635	O(10)-C(1)-C(2)	123.3457	C(10)-C(17)	1.4135	1.4168
C(1)-O(10)	1.3522	C(2)-C(15)-N(16)	178.6495			C(16)-C(17)	1.3952	1.3786
C(9)-O(10)	1.3930	C(7)-C(14)-C(13)	120.6013			C(15)-C(16)	1.3867	1.4130
C(4)-C(9)	1.3718	C(14)-C(13)-C(12)	120.2640			C(14)-C(15)	1.3948	1.3781
C(8)-C(9)	1.4260	C(8)-C(11)-C(12)	120.5083			C(4)-O(13)	1.3881	1.3658
C(7)-C(8)	1.4280	C(1)-O(10)-C(9)	118.9506			C(12)-O(13)	1.3803	1.3921
C(6)-C(7)	1.4350	O(10)-C(9)-C(4)	122.6719			C(7)-C(12)	1.3975	1.3743
C(5)-C(6)	1.3765	O(10)-C(9)-C(8)	114.9498			C(11)-C(12)	1.4138	1.4252
C(4)-C(5)	1.4221	C(4)-C(9)-C(8)	122.3764			C(10)-C(11)	1.4180	1.4284
C(3)-C(4)	1.5199	C(11)-C(8)-C(9)	122.6244			C(9)-C(10)	1.4178	1.4332
C(2)-C(3)	1.5213	C(11)-C(8)-C(7)	119.0327			C(8)-C(9)	1.3979	1.3776
C(1)-C(2)	1.3658	C(9)-C(8)-C(7)	118.3428			C(7)-C(8)	1.4030	1.4223
C(3)-H(27)	1.1004	C(14)-C(7)-C(8)	119.1438			C(6)-C(7)	1.5181	1.5204
		C(14)-C(7)-C(6)	121.9934			C(5)-C(6)	1.5033	1.5546
		C(8)-C(7)-C(6)	118.8628			C(4)-C(5)	1.3445	1.5163
		O(17)-C(6)-C(7)	114.9804			C(1)-O(3)	1.2274	1.2091
		O(17)-C(6)-C(5)	124.6737			C(1)-O(2)	1.3532	1.3440

Sup. Table 2: Optimized geometrical parameters of amino R-3b and imino S-3b at AM1 Semi-empirical using DFT/B3LYP with 6-311G* basis set.

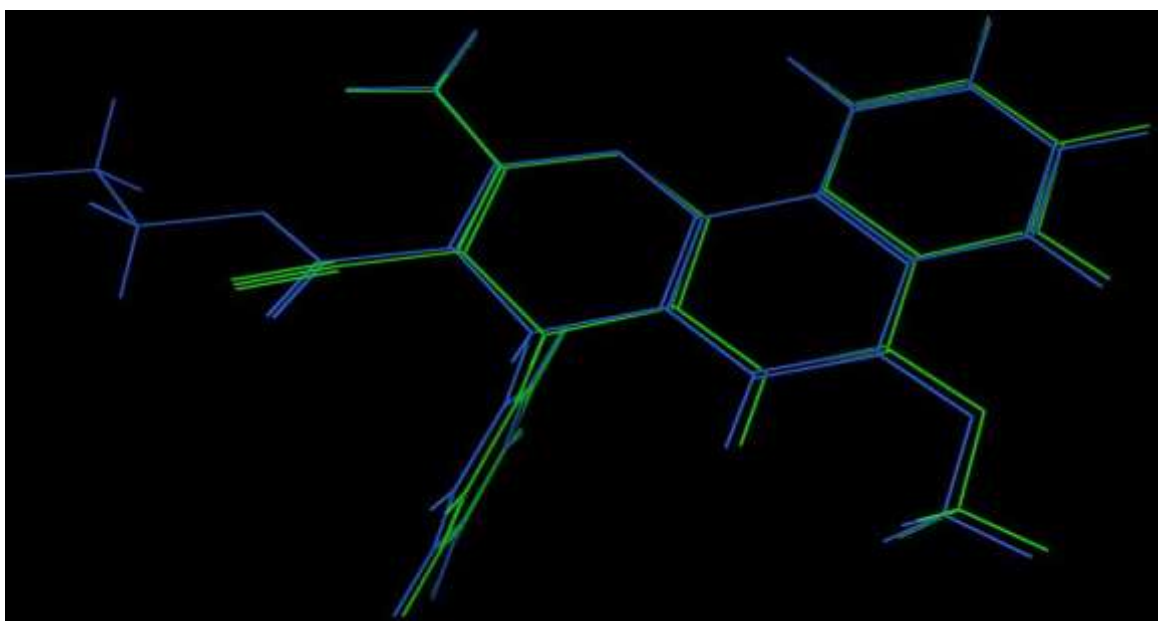
amino R-3b			Imino S-3b		
Atom Number	angle	angle	Atom Number	angle	angle
C(29)-C(28)-O(2)	106.9371	107.7768	C(10)-C(9)-C(8)	120.5055	120.0844
C(20)-C(25)-C(24)	121.2091	120.6947	C(9)-C(8)-C(7)	121.2737	120.8411
C(25)-C(24)-C(23)	119.0882	119.7723	C(12)-C(7)-C(8)	118.6278	119.25
Br(26)-C(23)-C(24)	119.4826	119.7758	C(12)-C(7)-C(6)	119.8998	120.2698
Br(26)-C(23)-C(22)	119.4234	119.7514	C(8)-C(7)-C(6)	121.4337	120.4773
C(24)-C(23)-C(22)	121.0924	120.4721	C(20)-C(6)-C(7)	113.9284	112.6494
C(23)-C(22)-C(21)	118.9738	119.7806	C(20)-C(6)-C(5)	110.0961	111.3515
C(22)-C(21)-C(20)	121.2993	120.663	C(7)-C(6)-C(5)	109.744	111.9737
C(6)-C(20)-C(25)	120.4572	119.5871	C(1)-C(5)-C(6)	109.552	114.9043
C(6)-C(20)-C(21)	121.191	121.7569	C(1)-C(5)-C(4)	109.5486	121.9802
C(25)-C(20)-C(21)	118.3357	118.6139	C(6)-C(5)-C(4)	112.5641	122.7918
C(9)-O(18)-C(19)	118.2352	117.8862	N(27)-C(4)-O(13)	121.1345	112.5567
C(10)-C(17)-C(16)	120.5858	121.8443	N(27)-C(4)-C(5)	121.5496	125.9596
C(17)-C(16)-C(15)	120.2889	119.7184	O(13)-C(4)-C(5)	117.2275	121.4802
C(16)-C(15)-C(14)	120.4453	119.6902	C(28)-O(2)-C(1)	122.84	123.5347
C(11)-C(14)-C(15)	120.511	121.6434	C(5)-C(1)-O(3)	120.9564	119.7707
C(4)-O(13)-C(12)	121.8597	120.3617	C(5)-C(1)-O(2)	119.5559	118.9846
O(13)-C(12)-C(7)	122.5762	121.4141	O(3)-C(1)-O(2)	119.4399	121.2444
O(13)-C(12)-C(11)	114.9821	117.3203			
C(7)-C(12)-C(11)	122.4092	121.2656			
C(14)-C(11)-C(12)	122.5301	122.1803			
C(14)-C(11)-C(10)	119.0349	118.7741			
C(12)-C(11)-C(10)	118.4349	119.0456			
C(17)-C(10)-C(11)	119.1339	118.3297			
C(17)-C(10)-C(9)	122.1292	122.1655			
C(11)-C(10)-C(9)	118.7369	119.5048			
O(18)-C(9)-C(10)	115.0317	116.1351			
O(18)-C(9)-C(8)	124.4617	123.7806			

Sup. Table 3: Mulliken $q(M)$ and electrostatic $q(el)$ and neutral charges $q(n)$ for S-3a and S-3b at AM1 Semi-empirical using DFT/B3LYP with 6-311G* basis set.

Atom	$q(M)$	$q(el)$	$q(n)$	Atom	$q(M)$	$q(el)$	$q(n)$	Atom	$q(M)$	$q(el)$	$q(n)$	Atom	$q(M)$	$q(el)$	$q(n)$
S-3a				H3	+0.123	+0.138	+0.245	S-3b				C24	-0.126	-0.151	-0.237
C1	+0.542	+0.554	+0.607	H4	+0.123	+0.134	+0.239	C1	+0.669	+0.526	+0.811	C25	-0.255	-0.183	-0.220
C2	-0.464	-0.107	-0.311	H5	+0.118	+0.134	+0.240	O2	-0.428	-0.451	-0.552	Br26	-0.098	-0.080	+0.068
C3	+0.156	-0.386	-0.228	H6	+0.113	+0.152	+0.253	O3	-0.505	-0.473	-0.582	N27	-0.898	-0.777	-0.859
C4	-0.017	+0.001	-0.047	H7	+0.167	+0.173	+0.230	O4	+0.455	+0.483	+0.551	C24	-0.126	-0.151	-0.237
C5	-0.407	-0.284	-0.282	H8	+0.152	+0.156	+0.205	C5	-0.428	-0.015	-0.301	C25	-0.255	-0.183	-0.220
C6	+0.293	+0.249	+0.365	H9	+0.149	+0.161	+0.209	C6	+0.113	-0.305	-0.276	Br26	-0.098	-0.080	+0.068
C7	-0.029	-0.016	-0.093	H10	+0.130	+0.144	+0.245	C7	+0.009	+0.131	-0.063	N27	-0.898	-0.777	-0.859
C8	+0.110	-0.033	-0.078	H11	+0.128	+0.157	+0.254	C8	-0.391	-0.279	-0.305	C28	+0.474	-0.047	-0.109
C9	+0.082	+0.197	+0.317	H12	+0.120	+0.155	+0.253	C9	+0.289	+0.328	+0.350	C29	-0.678	-0.452	-0.697
O10	-0.279	-0.374	-0.533	H13	+0.142	+0.143	+0.245	C10	-0.047	+0.083	-0.093	H1	+0.067	+0.176	+0.278
C11	-0.185	-0.167	-0.172	H14	+0.364	+0.342	+0.415	C11	+0.129	+0.084	-0.082	H2	+0.158	+0.140	+0.245
C12	-0.131	-0.185	-0.188	H15	+0.376	+0.357	+0.427	C12	+0.034	+0.215	+0.320	H3	+0.121	+0.137	+0.244
C13	-0.114	-0.183	-0.197					C13	-0.237	-0.577	-0.523	C28	+0.474	0.047	-0.109
C14	-0.150	-0.176	-0.156					C14	-0.187	-0.194	-0.207	C29	-0.452	0.678	-0.697
C15	+0.365	+0.034	+0.280					C15	-0.105	-0.128	-0.229	H1	+0.067	+0.176	+0.278
N16	-0.446	-0.233	-0.346					C16	-0.124	-0.127	-0.237	H2	+0.158	+0.140	+0.245
O17	-0.202	-0.349	-0.532					C17	+0.034	+0.215	+0.320	H3	+0.121	+0.137	+0.244
C18	-0.406	-0.464	-0.190					O13	-0.237	-0.577	-0.523	H4	+0.119	+0.131	+0.238
C19	+0.217	+0.089	-0.019					C14	-0.187	-0.194	-0.207	H5	+0.121	+0.132	+0.239
C20	-0.248	-0.194	-0.183					C15	-0.105	-0.128	-0.229	H6	+0.112	+0.150	+0.252
C21	-0.131	-0.162	-0.210					C16	-0.124	-0.127	-0.237	H7	+0.168	+0.171	+0.229
C22	+0.074	-0.081	-0.102					C17	-0.124	-0.196	-0.195	H8	+0.159	+0.156	+0.205
C23	-0.100	-0.167	-0.212					O18	-0.216	-0.517	-0.526	H9	+0.150	+0.159	+0.207
C24	-0.284	-0.174	-0.179					C19	-0.345	-0.216	-0.316	H10	+0.137	+0.148	+0.249
Br25	-0.086	-0.049	+0.066					C20	+0.213	+0.167	-0.035	H11	+0.129	+0.155	+0.253
N26	-0.770	-0.802	-0.773					C21	-0.202	-0.175	-0.221	H12	+0.132	+0.157	+0.254
H1	+0.063	+0.164	+0.267					C22	-0.140	-0.152	-0.240	H13	+0.155	+0.161	+0.254
H2	+0.153	+0.141	+0.246					C23	+0.087	+0.014	-0.135	H14	+0.404	+0.340	+0.413
												H15	+0.409	+0.352	+0.420



Sup. Fig1. Numbering compound according program number



Sup. Fig. 2. Alignment of the lowest energy of most stable compound S-3a (green) and amino form S-3b (blue).

How to cite this article:

Elhenawy .A, Mohamed M. H, El-Agrody M.A “Synthesis, characterization, stereochemistry and DFT study of 2-amino-4*H*-benzo[*h*]chromene derivatives” *J. Atoms and Molecules*, 3(6), 2013: 598 – 616.